FULL PAPER

DALTON

Oxovanadium(IV) complexes of the dipeptides glycyl-L-aspartic acid, L-aspartylglycine and related ligands; a spectroscopic and potentiometric study

João Costa Pessoa,*[a] Tamás Gajda,[b] Robert D. Gillard,*[c] Tamás Kiss,*[b] Susana M. Luz,[a] José J. G. Moura,[d] Isabel Tomaz,[a] João P. Telo[a] and Ibolya Török[e]

[a] *Instituto Superior Técnico, Departamento de Engenharia Química, Av. Rovisco Pais, 1096 Lisboa, Portugal. E-mail: pcjpessoa@alfa.ist.utl.pt*
[b] *Attila József University, Department of Inorganic and Analytical Chemistry, H-6701 Szeged, POB 440, Hungary*
[c] *Department of Chemistry, University of Wales, POB 912, Cardiff, UK CF1 3TB*
[d] *Centro de Química Fina, Universidade Nova de Lisboa, Quinta da Torre, 2825 Monte da Caparica, Portugal*
[e] *Research Group for Biocoordination Chemistry of the Hungarian Academy of Sciences, Attila József University, Department of Inorganic and Analytical Chemistry, H-6701 Szeged, POB 440, Hungary*

The equilibria in the systems VO^{2+} + L (L = Gly-L-Asp, L-Asp-Gly, *N*-acetyl-L-aspartic acid or succinic acid) have been studied at 25 °C and 0.2 mol dm^3 K(Cl) medium by a combination of potentiometric and spectroscopic methods (ESR, circular dichroism and visible absorption). Formation constants were calculated from pH-metric data with total oxovanadium(IV) concentrations of $(0.6–4) \times 10^{-3}$ mol dm^{-3} and ligand-to-metal (L:M) ratios of 2–8 (AspGly) or 4–15:1 (other systems). The position of the Asp residue in the peptide chain affects the co-ordination mode of the ligands: while in the GlyAsp system bis complexes start to form at pH less than 2, for AspGly only 1:1 complexes form, with relatively high CD signal. The co-ordination behaviour of *N*-acetyl-L-aspartic and succinic acids is similar. The results of potentiometric and spectroscopic methods are self consistent. Isomeric structures are discussed for each stoichiometry proposed and the results compared with those for L-aspartic acid and dipeptides with non-co-ordinating side chains.

Introduction

To model potential binding sites for the oxovanadium(IV) cation, complexation by several α-amino acids and simple peptides has been investigated.[1–21] For dipeptides containing Gly and/or Ala, at VO^{2+} concentrations of $\approx 10^{-2}$ mol dm^{-3}, the hydroxide precipitates at pH ≈ 4–5, even when using high amino acid : metal (L:M) ratios, *e.g.* 150–180:1, and at pH > 7.5–8 the hydroxide slowly dissolves to give brown solutions, indicating that oxovanadium(IV) is extensively hydrolysed. The present study of the systems VO^{2+} + L (L = Gly-L-Asp, L-Asp-Gly, *N*-acetyl-L-aspartic acid and succinic acid) combines the results of potentiometric and spectroscopic techniques (ESR, circular dichroism and visible absorption). These ligands, as compared with simple oligopeptides, are expected to be more efficient VO^{2+} binders, due to their extra carboxylate group. Part of this work has been presented in a preliminary form.[22]

Precipitation of VO(OH)$_2$ is clearly not so important in these systems, as was also the case for L-aspartic acid,[5] and much lower L:M ratios may be used. If lower oxovanadium(IV) concentrations are used *e.g.* $\approx (1–4) \times 10^{-3}$ mol dm^{-3}, results of pH-potentiometric titrations with L:M ratios of 1 to 15:1 up to pH ≈ 5.0–6.5 (depending on the ligand) may be used to calculate formation constants. Potentiometry must be ruled out for pH > ≈8; pK_a(NH$_3$$^+$) ≈ 8.4 and 8.0 for Gly-L-Asp and L-Asp-Gly, respectively, limiting the use of samples with high L:M ratios in the pH range 8–9, and oxovanadium(IV) is extensively hydrolysed, particularly at pH > 10. Further, the very high absorbance values (especially for 450 < λ < 650 nm) of the [(VO)$_n$(OH)$_m$] species present also preclude the use of visible

spectra. Minor oxidation of V^{IV} may also affect spectral measurements.

The ESR spectra may give important information about the groups co-ordinated to oxovanadium(IV).[23–26] The CD and ESR spectra for solutions containing L-Ala-Gly, Gly-L-Ala and L-Ala-L-Ala with high L:M ratios gave clear evidence of peptidic N$_{amide}$ co-ordination,[16] suggesting the formation of **1** (Y = H$_2$O or OH$^-$) as the important species contributing to these spectra in the pH range 7.5–8.5. The crystal-structure characterisation of [NEt$_4$][V^{V}O(O$_2$)(Gly-Gly)]·1.58 H$_2$O,[27] of [V^{IV}O(Gly-Tyr)(phen)][28] [Gly-Tyr = glycyl-L-tyrosinate(2−), phen = 1,10-phenanthroline] and of [NHEt$_3$][V^{IV}O(mpg)-(phen)][29] [H$_3$mpg = *N*-(2-sulfanylpropionyl)glycine], where NH$_2$, N$_{amide}$ and CO$_2$$^-$ are equatorial, and the isolation of [V^{IV}O(Gly-Gly)(phen)]·2CH$_3$OH and [V^{IV}O(Gly-Ala)(phen)]·CH$_3$OH,[29] and their characterisation by continuous wave ESR and ^{14}N electron spin echo envelope modulation also indicate that the dipeptides Gly-Gly and Gly-Ala are bonded as in **1**.
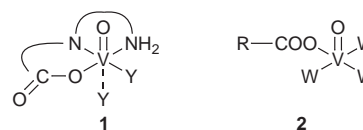
Circular dichroism (CD) spectra are more informative than the corresponding isotropic absorption spectra[30–33] for systems containing optically active amino acids and peptides. Only the vanadium–peptide complexes contribute to ΔA values (ΔA = differential absorption) in CD spectra, and the sign patterns

of Cotton effects can be compared for bands I, II (and III) of the different oxovanadium(IV) peptide and/or amino acid systems[23] as pH is varied. Since three pK_a values (terminal CO_2H, β-CO_2H of the aspartic side chain and terminal NH_3^+) can be determined for these dipeptides (H_3L^+), and two for the carboxylic groups of N-acetyl-L-aspartic acid and succinic acid (H_2L'), the formation constants correspond to the general reaction (1).

$$p\text{M}^{2+} + q\text{L}^{2-} + r\text{H}^+ \rightleftharpoons \text{M}_p\text{L}_q\text{H}_r \qquad (1)$$
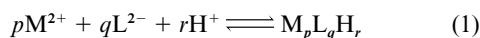
We abbreviate Gly-L-Asp as GlyAsp, L-Asp-Gly as AspGly and N-acetyl-L-aspartic acid as NacAsp. For the formulations $(\text{VO})_p(\text{ligand})_q\text{H}_r^{2p-2q+r}$ we normally use the abbreviation $\text{M}_p\text{L}_q\text{H}_r$ in the case of GlyAsp, AspGly and L-Asp, and $\text{M}_p\text{L}'_q\text{H}_r$ in the case of NacAsp, and other H_2L' ligands (e.g. alanine, succinic acid). For each $\text{M}_p\text{L}_q\text{H}_r$ or $\text{M}_p\text{L}'_q\text{H}_r$ proposed in our speciation models possible structures are discussed. Basicity corrected formation constants are used when needed to help in this discussion as in previous publications.[4,5,7,9]

Experimental

All solutions were prepared and manipulated in an inert atmosphere (high purity dinitrogen or purified argon). Amino acids (from Sigma) were dried for several days (in a desiccator with silica gel in vacuo), and succinic acid was a Fluka product of puriss p.a. quality for pH-metric studies and Merck p.a. (GR) for spectroscopic measurements. The KOH and HCl solutions used were Reanal products of the highest purity. KOH was standardized with potassium hydrogen phthalate and HCl with KOH potentiometrically. The purity of peptides was checked as described below and the exact concentrations of solutions were determined by the Gran method.[34] The experimental difficulties in the present systems were discussed in refs. 1 and 35. Stock solutions of VO^{2+} were prepared and standardised as described in ref. 1. The studies have been performed in 0.2 mol dm⁻³ K(Cl) ionic medium. For potentiometric measurements the temperature was 25.0 ± 0.1 °C, and for CD and VIS spectra 25.0 ± 0.3 °C.

TLC

Thin-layer chromatography was performed on Merck plates (Art. 5626, 10 × 20 cm). The compounds and solutions used for spectroscopic measurements were monitored throughout the whole pH range to check their purity and test for reactions (e.g. hydrolysis): neither contamination nor decomposition was detected. Usually 2 µl samples were applied to the plates and the eluent was butanol–ethanol–propionic acid–water (10:10:2:5). The chromatogram was developed with a ninhydrin–collidine (2,4,6-trimethylpyridine)–copper solution prepared according to Moffat and Lytle.[36] In some cases, after such development, the plate was placed in an enclosed chamber for development with iodine vapour. Typically, samples were taken for TLC after dissolution of the ligand, and addition of VO^{2+} at several pH values.

pH Measurements

Spectroscopic measurements. For preparation of the solutions and pH calibrations we used a special glass vessel with a double wall, with entries for the glass electrode (Orion Ross 81-01) and reference electrode (Orion Ross 80-05), thermometer, nitrogen and reagents (e.g. base). A computerised system developed locally (for an IBM-PCXT 286 computer) was used to control the titration conditions for pH calibrations. The emf measurements were made with a Crison 517 pH meter.

Potentiometric titrations. Stability constants were determined by pH-metric titration of 10.0 cm³ samples. The ligand concen-

tration was 0.004 and 0.008 mol dm⁻³ and ligand-to metal ion molar ratios: 2:1, 4:1, 6:1 and 8:1 (AspGly), and 2:1, 4:1, 6:1, 10:1 and 15:1 (other ligands). Titrations were performed from pH 2.0 until precipitation, very extensive hydrolysis or slow equilibration: these problems occurred in the pH range 5.0–6.7, depending on ligand and L:M ratio (see Table 1). Titrations were with KOH solution of known concentration (ca. 0.2 mol dm⁻³) under a purified argon atmosphere. In some cases pH equilibrium could not be reached within 10 min due either to precipitation or very slow complex formation. Those titration points were omitted. The reproducibility of the included points was within 0.005 pH unit over the whole pH range. The pH was measured with an Orion 710A precision digital pH meter equipped with an Orion Ross 8103BN type combined glass electrode, calibrated for hydrogen ion concentration as described earlier.[37] The ionic product of water was $pK_w = 13.76$. The concentration stability constants $\beta_{pqr} = [\text{M}_p\text{L}_q\text{H}_r]/[\text{M}]^p[\text{L}]^q[\text{H}]^r$ were calculated with the aid of the PSEQUAD computer program.[38] The formation of the hydroxo complexes of VO^{2+} was taken into account. The following species were assumed: $[\text{VO(OH)}]^+$ (log $\beta_{1-1} = -5.94$), $[\{\text{VO(OH)}\}_2]^{2+}$ (log $\beta_{2-2} = -6.95$), with stability constants calculated from the data of Henry et al.[39] and corrected for the different ionic strength using the Davis equation.

Spectroscopic measurements

The CD spectra were recorded with a JASCO 720 spectropolarimeter with a red-sensitive photomultiplier (EXWL-308), visible spectra with a Perkin-Elmer lambda 9 spectrophotometer. Unless otherwise stated, by visible (VIS) and circular dichroism (CD) spectra we mean a representation of ε_m or $\Delta\varepsilon_m$ values vs. λ [ε_m = absorption/bC_{VO} and $\Delta\varepsilon_m$ = differential absorption/bC_{VO} where b = optical path and C_{VO} = total oxovanadium(IV) concentration]. The spectral range covered was usually 400–900 (VIS) and 400–1000 nm (CD). The ESR spectra were usually recorded at 77 K with a Bruker ESR-ER 200D X-band spectrometer. The CD, VIS and ESR spectra for GlyAsp, NacAsp and succinic acid systems were recorded by varying the pH with approximately fixed total vanadium and ligand concentration, at L:M ratios of 15 and 30; for AspGly this was done for solutions with L:M = 9.8:1. Several CD and ESR spectra were also recorded at fixed pH at varying L:M ratios by addition of VO^{2+} stock solution. the GlyAsp solutions at pH 6.1 (L:M = 35.0, 24.7, 14.5, 9.4:1) as well as at 7.5 (35.0, 15.0, 9.4:1), 7.3 (20.1:1), and AspGly solutions at pH 4.9 (L:M = 10, 7.1, 6.3, 5.6, 4.6:1) as well as at 6.8 (L:M = 7.1:1) and 2.6 (L:M = 4.6:1) were used for these measurements.

Results and discussion

Protonation and formation constants calculated for the systems studied[38] are in Table 1. The protonation constants agree well with earlier results:[40–43] the presence of the N-acetyl group in NacAsp increases the acidity of the CO_2H groups relative to succinic acid.

These ligands all contain two carboxylate binding sites and VO^{2+} has a strong affinity for oxygen containing ligands,[23] so their complexes may differ from those of simple dipeptides such as GlyGly, AlaGly, GlyAla or AlaAla.[16] Further, relatively low L:M ratios (e.g. 10:1) may be adequate to avoid precipitation of $VO(OH)_2$ in the case of GlyAsp and AspGly. Complexation starts through monodentate carboxylate co-ordination (as in **2**): MLH_2 for GlyAsp and AspGly (one proton belongs to the terminal NH_3^+, the other to the non-co-ordinated CO_2H group) and ML'H for NacAsp and succinic acid (the proton belongs to the non-co-ordinated CO_2H group). With high excesses of ligand, the bis complexes $M(LH_2)_2$ or $M(L'H)_2$ may also be formed. However, their formation can hardly be detected by pH-metry due to the overlap between the pro-

**Table 1** Formation constants (log values[a]) of species formed in VO²⁺–ligand systems at $T = 298$ K and $I = 0.2$ mol dm⁻³ KCl

$M_pL_qH_r$	GlyAsp	AspGly	$M_pL'_qH_r$	NacAsp	Succinic acid
HL⁻	8.36(1)	7.93(1)	HL'⁻	4.52(2)	5.19(1)
H₂L	12.58(2)	11.50(2)	H₂L'	7.61(5)	9.17(3)
H₃L⁺	15.24(3)	14.32(3)			
pK_{a1}	2.66	2.82	pK_{a1}	3.09	3.98
pK_{a2}	4.22	3.57	pK_{a2}	4.52	5.19
pK_{a3}	8.36	7.93			
MLH₂²⁺	15.1(5)	13.4(2)	ML'H⁺	6.2(2)	7.2(2)
MLH⁺ [b]	11.52(8)	10.46(3)	ML' [b]	2.7(2)	3.20(4)
ML		6.42(2)			
MLH₋₁⁻	1.7(1)	0.83(4)	ML'H₋₂²⁻	−7.32(5)	−7.25(3)
ML₂H₃⁺ [b]	26.6(2)		ML'₂H⁻ [b]	9.56(6)	10.76(4)
ML₂H₂	22.5(3)		ML'₂²⁻	5.0(3)	5.6(1)
ML₂H⁻	17.1(2)				
pH range studied	2.0–5.5	2.0–5.5		2.0–6.2	2.0–6.7
L:VO ratio	4–15	2–8		4–15	4–15

[a] Formation constants correspond to $\beta_{pqr} = [M_pL_qH_r]/[M]^p[L]^q[H]^r$ where L is the ligand in its deprotonated form (L²⁻). Oxovanadium(IV) hydrolysis products are VO(OH)⁺ and [(VO)₂(OH)₂]²⁺ with log $\beta_{10-1} = -5.94$ and log $\beta_{20-2} = -6.95$. The numbers in parentheses apply to the last digit included; it defines the range of log β values in refinements with PSEQUAD for the several plausible models obtained. [b] Formation constants for stoichiometries MLH (or ML') and ML₂H₃ (or ML'₂H) could not be refined simultaneously (see text).

cesses of co-ordination and deprotonation of the carboxylate group and to the high buffering effect of large excesses of ligand. Accordingly, most of the resultant pH change belongs to ligand deprotonations and only a relatively small part to VO²⁺ complexation.

It is also worth mentioning that β_{111} and β_{123} could not be refined simultaneously; if both were included in the same calculation; one was always rejected, even if only data obtained at high excesses of ligand were included in the calculation. Probably ML₂H₃ does not exist in significant concentration at low L:M and the same applies to MLH at high L:M. For the corresponding stoichiometries ML' and ML₂'H for the NacAsp and succinic acid systems, it was similarly not possible to refine β_{110} and β_{121} simultaneously. This is because, in the pH range 3–4.5 in which bis complexes are mostly formed, the ligand has already lost a proton from its more acidic carboxylic function, hence the complex formation involves no H⁺, eqns. (2A) and (2B). Under the conditions used for pH-

$$VOLH⁺ + H₂L \rightleftharpoons VOL₂H₃⁺ \quad (2A)$$

$$VOL' + HL'⁻ \rightleftharpoons VOL'₂H⁻ \quad (2B)$$
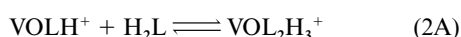
potentiometry (except for AspGly) the formation of 2:1 species is assumed above pH ≈ 2–3; when using high L:M, no polymeric complexes are expected till pH ≈5. Fig. 1 gives calculated[44] distributions of concentration.

The X-band ESR spectra of frozen 'solutions' may be simulated as axial spectra. The field region corresponding to $A_∥$ and $M_I = 5/2$ and $7/2$ gives more information about the type and number of species. Fig. 2 shows ESR spectra in this range. When the pH is increased from ≈1 to ≈3.2 (AspGly), to ≈3.5 (GlyAsp), to ≈5.0 (NacAsp) or to ≈ 6.5 (succinic acid, not seen), the peaks shift slightly to lower field, so more than one species contribute to each spectrum. For higher pH, distinct species are detected, but for pH > 6–7 (for NacAsp and succinic acid) or > 8 (for GlyAsp or AspGly) the signal weakens significantly, increasing again at pH > 12, due to the formation of VO(OH)₃⁻. For VO²⁺ and succinic acid with L:M = 30:1 and C_{VO} ≈ 0.008 mol dm⁻³, a new component appears from pH > ≈6.7; it may correspond to ML'H₋₃ (or indeed another stoichiometry, e.g. ML'₂H₋₂/₋₃). At pH 7.3 the components ascribed to ML'H₋₂ and ML'H₋₃ have relative intensities approximately 3:2. At pH 7.9 most VO²⁺ is precipitated and the ESR signal is weak. Table 2 summarizes the spin Hamiltonian parameters obtained by simulating the whole spectrum using program EPRPOW,[45] ascribing the ESR-active components to

specific stoichiometries. Superscripts 'exptl' and 'est' refer to 'experimental' and estimated parameters [eqn. (3)] where $A_{∥,i}$

$$A_∥^{est} = \sum_{i=1}^{4} A_{∥,i}/4 \quad (3)$$

are the contributions to $A_∥^{est}$ of each of the four equatorial groups (most presented by Chasteen[24] with estimated accuracy ±3 × 10⁻⁴ cm⁻¹).

Fig. 3 includes visible spectra for (A) GlyAsp + VO²⁺ with L:M ratio 30:1 and (B) AspGly + VO²⁺ with L:M ratio 9.8:1. For pH < 2.5, they resemble (except for ε_m values) oxovanadium(IV) solutions. Visible spectra for NacAsp or succinic acid + VO²⁺ are similar and show the same trend as V^IVO–GlyAsp. For pH > 2.5, as pH increases, band II gradually separates from band I revealing a progressive increase of the ligand field around VO²⁺. However, while spectra for solutions of GlyAsp, NacAsp or succinic acid + VO²⁺ are similar and their changes are like those found for dipeptides with non-co-ordinating side chains, the spectra for AspGly + VO²⁺ differ: band II shifts ≈30–40 nm to the UV and its ε_m values are about the same as those for band I. This means that the type of complexes formed and their co-ordination geometries differ in the system with AspGly. In the pH range 1–4.5 the VIS spectra for solutions of AspGly resemble those for L-Asp.[5]

The CD spectra for the GlyAsp, AspGly and NacAsp systems modify as the pH is increased. In the pH range 1.5–5, all differ from those for L-Asp.[5] Fig. 4 includes spectra for (A) GlyAsp + VO²⁺ with L:M 15:1 and (B) AspGly + VO²⁺ with L:M 9.8. In the pH range 1–4, CD spectra of NacAsp + VO²⁺ with L:M 30:1 are similar and show the same trend as those of GlyAsp: maximum values of $\Delta\varepsilon_m$ for band I are found in the pH range 4.1–4.6. The decrease in intensity of this band for pH > 4.8 is apparently due to the formation of ML'₂ and is more significant when ML'H₋₂ forms [Fig. (1C)].

For pH > 4.5 the CD spectra for GlyAsp, AspGly and NacAsp differ (Fig. 5) and also modify as pH is increased. For pH > 10 optical activity is low and becomes almost zero for pH > 11. The pattern of the CD bands and approximate λ_{max} values ascribed to each stoichiometry and comparison with species distribution is in Table 2. The CD (e.g. Fig. 5) and ESR (Fig. 2) spectra of VO²⁺ + GlyAsp in the pH range 8–9.5 have the same profile and very similar spin-Hamiltonian parameters as those for simple dipeptides such as GlyAla, AlaAla, etc.[16] As with them, this GlyAsp complex probably involves N_{amide} equatorial co-ordination. While for GlyAsp with L:M 30:1,
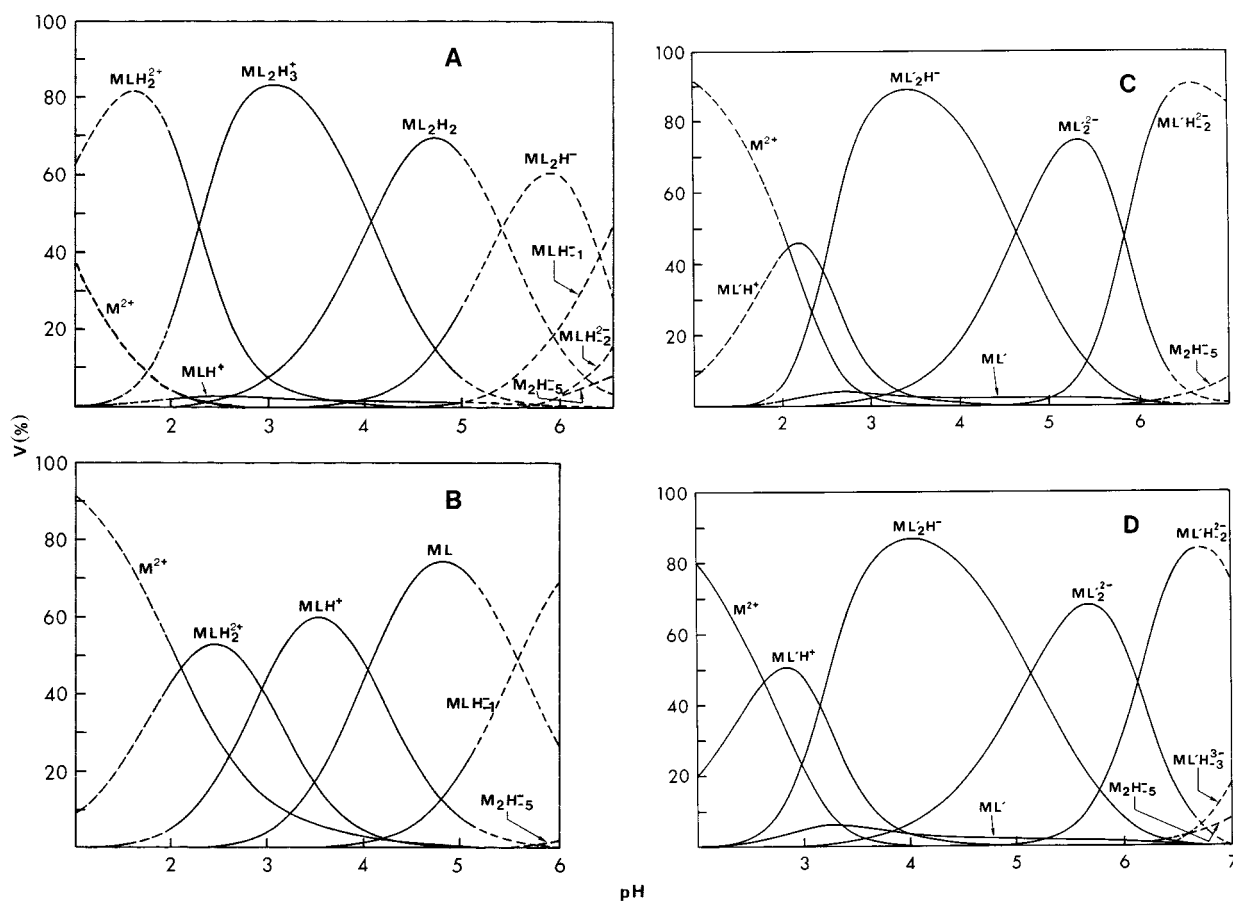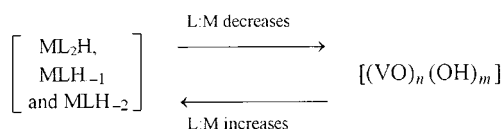
Fig. 1 Concentration distribution of the complexes formed in the (A) GlyAsp–, (B) AspGly–, (C) NacAsp– and (D) succinic acid–VO^{2+} systems in solutions with $C_{VO} = 0.008$ mol dm^{-3} and L:M = 10 (AspGly) or 30:1 (other systems), calculated[44] using β_{pqr} of the equilibrium models of Table 1. The dashed lines indicate that the curves only represent an approximate estimation of the relative concentrations. The possible relative proportion of $[(VO)_m(OH)_n]$ hydrolysis products is estimated assuming the formation of M_2H_{-5} with $\beta_{2-5} = 10^{-21.8}$.[1,23] For MLH_{-2} (GlyAsp) and $ML'H_{-3}$ (succinic acid) no β values are available, and concentrations were roughly estimated from the ESR spectra.

maximum $|\Delta\varepsilon_m|$ values are for pH ≈ 9.5, for AlaAla and GlyAla these are at pH ≈ 7.5.

The CD and ESR spectra have also been recorded at fixed pH for varying but high L:M ratios. The profile for the grey solution containing GlyAsp + VO^{2+} at pH 6.1 with L:M = 35:1 and $C_{VO} = 6.0 \times 10^{-3}$ mol dm^{-3} is very similar to spectrum 2 in Fig. 5(A), but the $|\Delta\varepsilon_m|$ are ≈ 1.5 times larger. The corresponding ESR spectrum is like that in Fig. 2(A) (pH 5.97). On adding VO^{2+} stock solution till L:M = 9.4:1 the solution becomes greenish (L:M = 24.7:1) and dark green (L:M = 14.5 or 9.4:1); the CD and ESR spectral profiles remain the same but the ESR signal increases and values of $|\Delta\varepsilon_m|$ decrease: at L:M = 9.4:1 to $\approx 20\%$ of those for L:M = 35:1. These significant changes in $\Delta\varepsilon_m$ as C_{VO} is varied can be explained only by equilibria between species with different degrees of polymerisation. At pH 6.1 these could be as in Scheme 1.

$$\begin{bmatrix} ML_2H, \\ MLH_{-1} \\ \text{and } MLH_{-2} \end{bmatrix} \xrightleftharpoons[\text{L:M increases}]{\text{L:M decreases}} [(VO)_n(OH)_m]$$

Scheme 1 Equilibria and main species involved at pH ≈ 6.1 in the GlyAsp system.

As long as the L:M ratios are high (*e.g.* $> 12:1$) the relative concentrations of monomeric complexes vary little with C_{VO} but the % of vanadium in the form of monomeric *vs.* oligomeric species varies significantly. Since the pattern of the CD spectra changes little with C_{VO} (and ill defined isodichroic points are observed at $\lambda \approx 560$ and 790 nm with $\Delta\varepsilon_m \approx 0$), the oligomeric species present at pH 6.1 must be optically inactive. Other

amino acid systems behave similarly.[1–6] In similar experiments at pH 7.5, when extra VO^{2+} was added to a sample of L:M = 35:1 (light yellowish brown) to change L:M to $\approx 14.5:1$ (pH 7.50, dark green) the CD profile changed, in particular, the Cotton effect associated with the band at 700 nm became negative and the band at *ca.* 800 nm shifted to the red. Overall $|\Delta\varepsilon_m|$ decrease to $\approx 30\%$ of those for L:M = 35:1. On addition of more VO^{2+} till L:M = 9.4:1 (pH 7.50, very dark green), the CD spectrum becomes very noisy but now the profile apparently changes little. The ESR profile for these experiments at pH 7.5 is always the same: the dominant components are those designated by MLH_{-1} and/or MLH_{-2}. Therefore at this pH the changes in CD profile and $\Delta\varepsilon_m$ with C_{VO} can be explained only by assuming equilibria between monomeric complexes (MLH_{-1} and MLH_{-2}), optically and ESR active, and oligomeric species (*e.g.* $M_2L_2H_{-3}$, $M_2L_2H_{-4}$) which are optically active but ESR-inactive. Optically inactive oligomeric species, *e.g.* $[(VO)_n(OH)_m]$, probably also have significant concentrations at pH 7.5. Scheme 2 summarizes the processes expected to occur as pH is increased.

For GlyAsp + VO^{2+} the distribution of Fig. 1(A) describes the ESR spectra of Fig. 2(A) reasonably well till at least pH ≈ 6.

$$ML_2H \longrightarrow \begin{bmatrix} MLH_{-1} + MLH_{-2} \\ + \\ \text{optically active oligomeric species} \\ + \\ \text{optically inactive oligomeric species} \end{bmatrix} \longrightarrow MH_{-3}$$
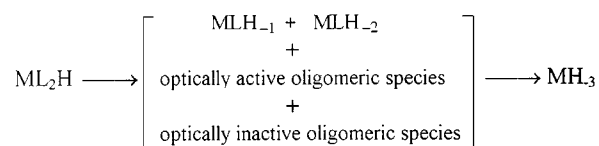
Scheme 2 Overall description of processes as pH is increased in the range 6.5–13 for the GlyAsp system. The optically active oligomeric species is expected to form in the pH range 6.5–10.
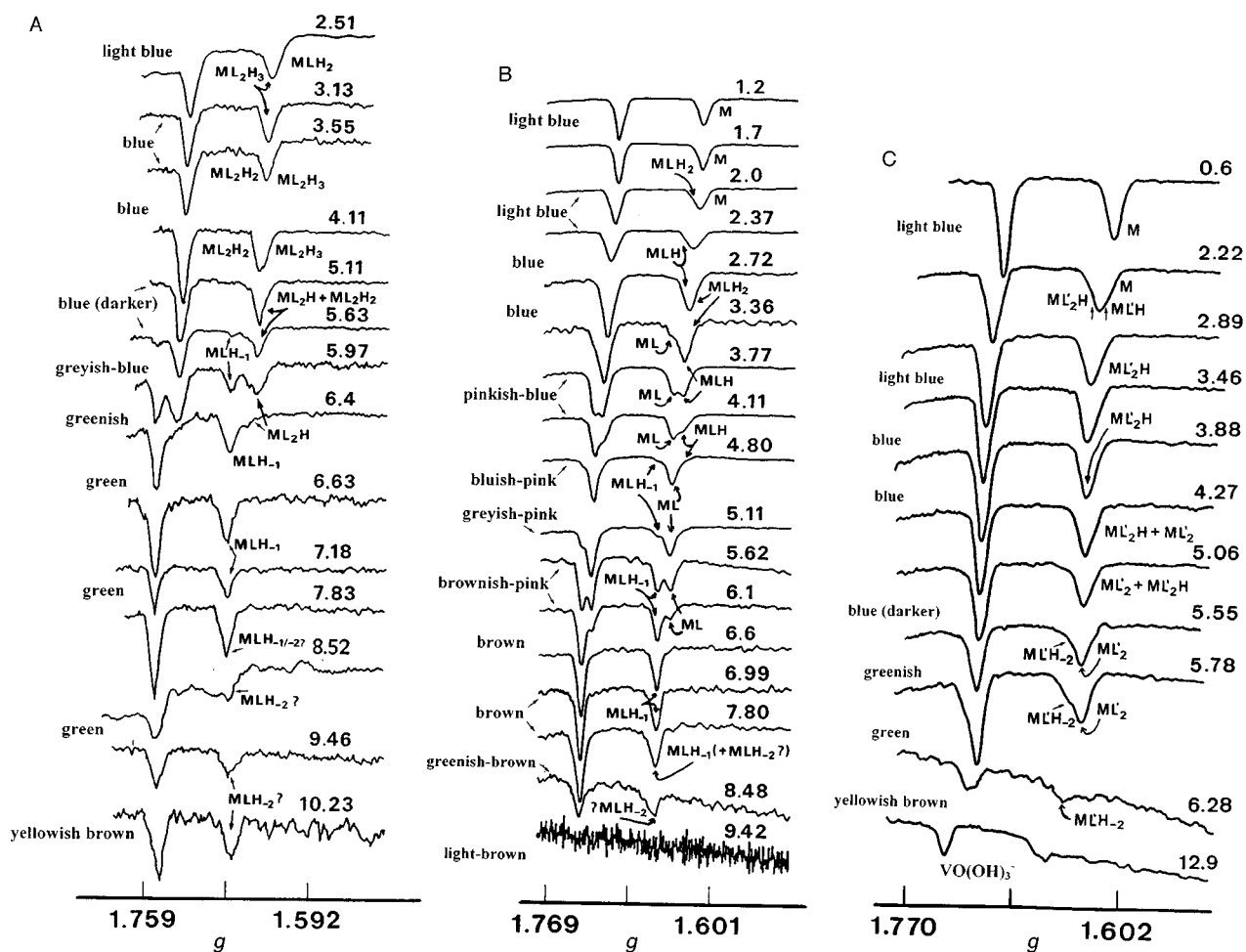
Fig. 2 High field range (3800–4400 G) of the first derivative ESR spectra at 77 K of frozen "solutions" containing (A) GlyAsp and VO^{2+} with L:M = 30.0:1 and $C_{VO} \approx 0.008$–0.011 mol dm^{-3}, (B) AspGly and VO^{2+} with L:M = 9.8:1 and $C_{VO} \approx 0.006$–0.010 mol dm^{-3} and (C) NacAsp and VO^{2+} with L:M = 30.0:1 and $C_{VO} \approx 0.008$–0.014 mol dm^{-3}. pH Values, colours of the corresponding solutions and stoichiometries corresponding to the ESR components are indicated.

For pH > 6–6.5 at least two different ESR-inactive oligomers form, as well as an ESR and CD active complex: possibly MLH_{-2}. Some results for it are in Table 2. No value of β is available and its concentration in Fig. 1(A) was roughly estimated from the ESR results. For AspGly + VO^{2+}, till at least pH 6 the distribution of Fig. 1(B) also describes reasonably well the relative intensities of the ESR-active species in Fig. 2(B). The CD signal is weak and noisy under conditions corresponding to these ESR spectra for pH < 2.7. At pH 1.2 $VO(OH_2)_5^{2+}$ predominates and for pH < 1.7 the dominant optically active species is MLH_2, with negative $\Delta\varepsilon$, as for amino acid complexes containing a mono-co-ordinated carboxylate function.[1–8,16] Since the CO_2^- group is now from an achiral glycine residue the CD signal is very weak. The structure of this complex probably corresponds to **3** (Table 3) so the vicinal effect is transmitted mainly through the axial $(NH)C=O_{amide}$, not as efficient as an equatorial CO_2^- group.[16] For pH > ≈2.0 $\Delta\varepsilon_m$ becomes positive due to the formation of MLH. The CD profile in the pH range 2.7–4.1 is approximately the same so the relevant spatial factors that determine the CD signal are similar for MLH and ML. Although the VIS spectra of solutions containing AspGly and VO^{2+} for pH > 3 suggest increased ligand field strength, no such increase occurs for GlyAsp or NacAsp. This suggests that in ML the NH_2 group is also co-ordinated (e.g. **12** and **13** in Table 3).

For AspGly and VO^{2+} with L:M = 9.8:1, at pH 6 [Fig. 5(B)], the overall CD signals are intense with the band pattern: +,+,− for bands II, IB, IA and: $\Delta\varepsilon_m^{band\ II} \approx 2\Delta\varepsilon_m^{band\ IB} \gg \Delta\varepsilon_m^{band\ IA}$. As pH is increased in the range 6–8 the

pattern changes to +,+,+, bands II and IA now being about equal. These modifications indicate that besides MLH_{-1} a new optically active species forms. In the same pH range the ESR signal decreases: in the range 8–10.5 oligomeric ESR inactive species {e.g. $[(VO)_n(OH)_m]$} form, causing further decrease. The spin-Hamiltonian parameters for the ESR-active species correspond to MLH_{-1} (Table 2). For AspGly + Cu^{II}, bis complexes formed, presumably involving amino acid-like co-ordination.[41] Our pH-metric results (till L:M = 8:1) suggest no formation of bis complexes till at least pH 5.2. The CD decreases for pH > 5 which indicates no significant formation of bis complexes at higher pH. Therefore, the ESR and CD active complex that forms for pH > 5–6 probably corresponds to a stoichiometry MLH_{-2}.

For NacAsp + VO^{2+} it is not straightforward to compare the distribution of Fig. 1(C) with the ESR [Fig. 2(C)] because $ML'H$, ML'_2H and ML'_2 cannot be detected separately. However, the agreement is reasonable: e.g. at pH 5.78 the distribution predicts ≈55% of ML'_2 and ≈37% of $ML'H_{-2}$, and this is in good accord with the intensities of the ESR components. The CD and VIS profiles for the solutions containing NacAsp corresponding to the ESR spectra of Fig. 2(C) at pH < 3.5 are very similar to those for GlyAsp under similar conditions. The main contributors to CD are $ML'H$ and ML'_2H. These correspond to stoichiometries MLH_2 and ML_2H_3 in the GlyAsp system. So, dominant factors that contribute to the optical activity must be similar for the corresponding complexes. For pH > 4 the CD spectra for GlyAsp and NacAsp differ. For NacAsp + VO^{2+} [Fig. 5(C)] the pattern of the CD is the same in the pH

Table 2 Hyperfine coupling constants, g values, λ_{max} of CD spectra (and corresponding signal) or of VIS spectra (and corresponding ε value for succinic acid) for several stoichiometries of each of the systems studied. Most A and g values were obtained by simulation with the program EPRPOW[45] of EPR spectra of frozen "solutions" at 77 K

Stoichiometry	$A_\parallel^{exptl} \times 10^4$	$g_\parallel^{exptl}$	$A_\perp^{exptl} \times 10^4$	$g_\perp^{exptl}$	λ_{max} (CD signals or ε)[a] band II	band I[b]
GlyAsp						
$MLH_2^{2+\,c}$	≈177	≈1.936	≈65.0	≈1.978	590 (−)	760 (−)
$ML_2H_3^+$	174.0	1.938	63.0	1.977	600 (−)	820 (−)
$ML_2H_2^{\,c}$	≈172	≈1.940	≈61	≈1.975	550 (−)	820 (−)
$ML_2H^{-\,c}$	≈171	≈1.942	≈60	≈1.977	?? (−)	??? (+), ??? (−)[d]
MLH_{-1}^-	160.7	1.953	53.5	1.981	≈510 (−)	730 (+)
					510 (−)	? 700 (+),[e] 850 (−)[e] ?
$MLH_{-2}^{2-\,c}$ (?)	162.5	1.951	53.7	1.985	510 (−)	730 (+)
AspGly						
$M^{2+\,f}$	181.2	1.934	68.2	1.978		
$MLH_2^{2+\,c}$	≈177.0	≈1.937	≈65–66	≈1.977	??? (−)	??? (−)[d]
$MLH^{+\,c}$	173.5	1.939	62.8	1.977	575 (+)	750 (+)
ML	169.8	1.944	60.8	1.977	565 (+)	730 (+)
MLH_{-1}^-	165.0	1.950	57.5	1.979	550 (+)	700 (+), 860 (−)
$MLH_{-2}^{2-\,c}$ (?)	163.5	1.949	54.0	1.980	525 (+)	735 (+). ≈880 (+)
NacAsp						
$M^{2+\,g}$	181.5	1.934	68.8	1.978		
$ML'H^{+\,c}$	≈177	≈1.937	≈65.2	≈1.977	610 (−)	770 (−)
ML'_2H^-	173.5	1.938	62.4	1.977	600 (−)	810 (−)
$ML'_2^{2-\,c}$	≈172	≈1.940	≈61.5	≈1.978	575 (+)	813 (−)
$ML'H_{-2}^{2-\,c}$ (?)	≈168	≈1.945	≈60.0	≈1.977	570 (+)	810 (−)
$MH_{-3}^{-\,h}$	162	1.955	49.5	1.977		
Succinic acid[i]						
$M + ML'H^+$ (pH 2.2)	179	1.934	69	1.978	??[d]	768 (19.0)
$M + ML'H^+ + ML_2'H^-$ pH 3.0	178	1.938	67	1.980	??[d]	773 (22.6)
$ML_2'H^-$	174	1.940	63	1.981 pH 3.80	≈625 (≈12)	780 (26.1)
ML'_2^{2-}	172	1.942	61	1.980 pH 5.75	605 (18.5)	800 (32.5)
$ML'H_{-2}^{2-}$	172	1.942	61	≈1.980 pH 6.32[j]	565 (21)	830 (23.0)
	171	1.942	61	≈1.980 pH 6.95[j]	565 (113[k])	830 (64[k])
$ML'H_{-3}^{3-}$ (?)	≈165	≈1.944	≈62	≈1.982		

[a] Based on qualitative analysis of experimental CD spectra and distribution diagrams. For succinic acid the λ_{max}/nm and ε_m/dm^3 mol^{-1} cm^{-1} presented are those for VIS spectra at pH values where each stoichiometry is expected to be largely predominating. [b] When splitting of band I is clearly observed, two λ_{max} values are given: bands IB and IA. [c] The ESR spectrum was difficult to simulate due to noise or presence of a significant amount of more than one species. [d] The λ_{max} cannot be estimated satisfactorily. [e] This species could have this pattern or the same as for MLH_{-2} (see text). [f] From ESR spectra of solutions containing AspGly and VO^{2+} (L:M = 9.8 and $C_{VO} \approx 0.010$ mol dm^{-3}) at pH 1.0 and 1.2. [g] From ESR spectra of solutions containing NacAsp + VO^{2+} (L:M = 30 and $C_{VO} \approx 0.010$ mol dm^{-3}) at pH 0.6 and 1.2. [h] From the ESR spectra of a solution containing NacAsp and VO^{2+} at pH 12.9 (L:M = 30 and $C_{VO} \approx 0.008$ mol dm^{-3}). [i] Each spectrum seems to correspond to only one component, but all correspond to at least two species. Only parameters for ML'_2H, ML'_2, $ML'H_{-2}$ can be determined with reasonable accuracy. [j] The λ_{max} and ε for $ML'H_{-2}$ are only rough approximations as at pH 6.32 the contribution of oligomeric species e.g. $[(VO)_n(OH)_m]$ is significant. [k] The ε_m of solutions containing succinic acid and VO^{2+} (L:M = 30 and $C_{VO} \approx 0.008$ mol dm^{-3}) at pH $\approx$ 7 decreases continuously from 350 ($\varepsilon \approx 606$) to 900 nm ($\varepsilon_m \approx 61$ dm^3 mol^{-1} cm^{-1}). Here ε_m values are given at 565 and 830 nm, the λ_{max} observed at pH 6.32.

range 4.2–6.3, with λ_{max} 550–580 (band II) and 805–815 nm (band I), see Table 2. The value of $|\Delta\varepsilon_m|$ increases till pH ≈4.7 (band I) or 5.8 (band II). At pH > 3.5, for NacAsp $\Delta\varepsilon_m > 0$ in the region of band II, but negative till pH ≈6.7 for GlyAsp. Formation constants could be calculated from titrations up to pH 6.2 (Table 1) but the ESR of Fig. 2(C) and the CD of Fig. 5(C) reflect no new ESR or CD active complexes till pH ≈ 9.3. However, intensities decrease markedly for pH > 7 indicating the formation of $[(VO)_n(OH)_m]$ inactive in ESR and CD. So Fig. 1(C) includes $[\{(VO)_2(OH)_5^-\}_m]$ with $m = 1$, in accord with previous practice,[1–9] but in reality m is probably more than 1.

The ESR and VIS spectra for VO^{2+}–succinic acid at high L:M as pH is varied resemble those for NacAsp but at pH > ≈3.5 bands I and II are more distinctly separate. This system was previously studied by spectroscopic[18,46] and pH-potentiometric[43,46] methods at L:M ratios of 1 and 2:1, and by ESR[47] using L:M 100:1. The formation of a single complex ML' (with stability constant 10$^{3.66}$) was assumed at 30 °C and $I = 0.1$ mol dm^{-3} KNO$_3$.[43] At low excess of ligand, in the pH range 4.5–6, spectroscopy (VIS and ESR) gave evidence only for the monodentate carboxylato complex **2**, besides the aqua ion and VO^{2+} hydroxo complexes. It was characterised by

absorption maxima at 590–600 (band II) and 780–810 nm (band I).[18,46] Our VIS spectra at high excess of ligand show features apparently not then observed[18,46] at low L:M ratios. Two bands are distinct in the range 450–900 nm for pH > 3.5, with λ_{max}(band II) ≈565 nm and λ_{max}(band I) ≈830 nm: this suggests complexes with bidentate succinate (or the mono-dentate co-ordination of three or more succinate ligands). The conclusions of Ferrari *et al.*[18] based on ESR and VIS spectra are similar, except that they assumed **2** to form at lower pH. In their ESR study with $C_{VO} = 10^{-3}$ mol dm^3 and L:M 100:1, McPhail and Goodman[47] detected four components in the pH range 3–6, finding A to decrease and g to increase as pH is increased. Our ESR results agree.

With succinic acid at high L:M the distribution of Fig. 1(D) describes the spectroscopic results up to pH 6.7. The new ESR-active species at pH ≈7 could correspond to a ML'H$_{-3}$ stoichiometry: its estimated spin-Hamiltonian parameters are in Table 2. As at least two distinct components are detected in the ESR spectra; the parameters were obtained by simulation of spectra but using equations[48] based on Chasteen's[24] iterative method. Lacking a β value, the relative concentration was estimated from ESR.
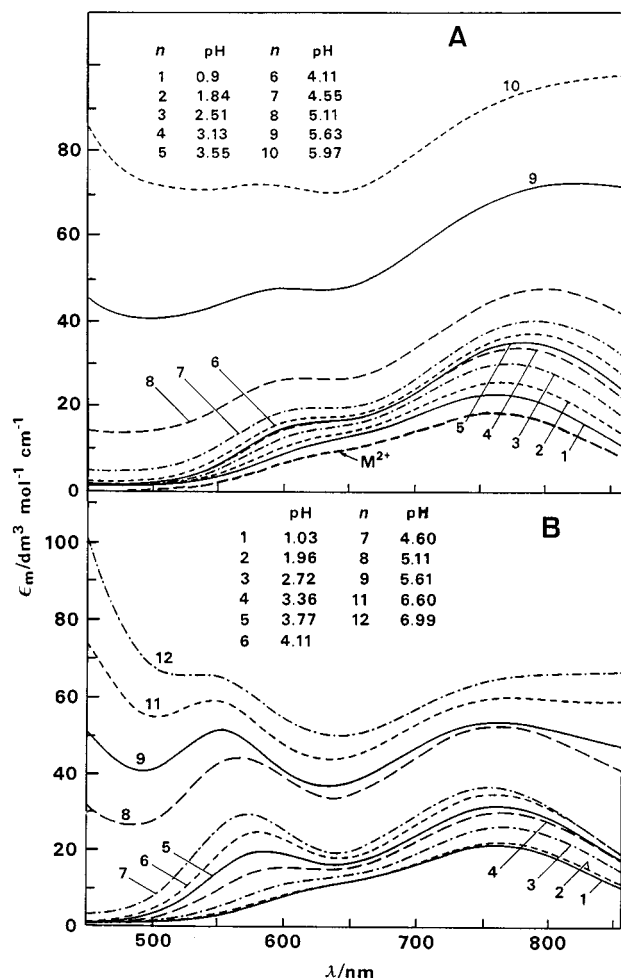
Fig. 3 Visible absorption spectra of solutions containing (A) GlyAsp and VO^{2+} with $L:M = 30.0:1$ and $C_{VO} \approx 0.008–0.011$ mol dm^{-3} and, (B) AspGly and VO^{2+} with $L:M = 9.8:1$ and $C_{VO} \approx 0.006–0.010$ mol dm^{-3}. The pH corresponding to each spectrum is indicated. Spectrum 1 in B approximately coincides with that of $VO(OH_2)_5^{2+}$ ($\equiv M^{2+}$). The ESR spectra corresponding to some of these solutions are in Fig. 2.

Fig. 4 Circular dichroism spectra of solutions containing (A) GlyAsp and VO^{2+} with $L:M = 15.0:1$ and $C_{VO} \approx 0.018–0.020$ mol dm^{-3} and, (B) AspGly and VO^{2+} with $L:M = 9.8:1$ and $C_{VO} \approx 0.008–0.010$ mol dm^{-3}. The pH corresponding to each spectrum is indicated. The ESR and VIS spectra corresponding to some of the AspGly solutions are in Figs. 2 and 3.

Since the vanadyl ion is lop-sided many of its chelates may give rise to more isomers than do those of apparently analogous monoatomic metal centres such as Cu^{II} refs. 1 and 23 briefly discuss this. For monodentate ligands, such as an amino acid bonded *via* its carboxylate, this extra isomerism would be absent. However, if there are two such ligands geometric isomers may be present. We now discuss, on the basis of Figs. 2–5 and Tables 1 and 2, the dominant structure in solution for each stoichiometry. For a given stoichiometry and similar co-ordination geometry, CD spectra for GlyAsp, AspGly and NacAsp may differ.

Table 3 gives plausible structures and, for each, the main mechanisms for inducing optical activity. These systems are labile. Optical activity consequently arises from the chiral arrangement of the chelate rings, *i.e.* the *conformational effect*,[30] and, since the ligands contain asymmetric carbon atoms, from the transmission through space and by way of the chemical bonds linking the asymmetric centre to the chromophore, *i.e.* the *vicinal effect*.[30] The order of magnitude of the conformational effect depends on the chelate-ring puckering and that of the vicinal effect on the number of atoms between the asymmetric centre and the metal, and on the efficiency of the donor groups in transmitting dissymmetry, which for peptides has been suggested to be:[16,31] $N_{amide} > (CO)N_{amide} > CO_2^- > C=O_{amide} > (NH)C=O_{amide} > NH_2$. We also assume here and elsewhere[1–8,16] that optical activity transmits better from chiral centres of the ligand into optical transitions through
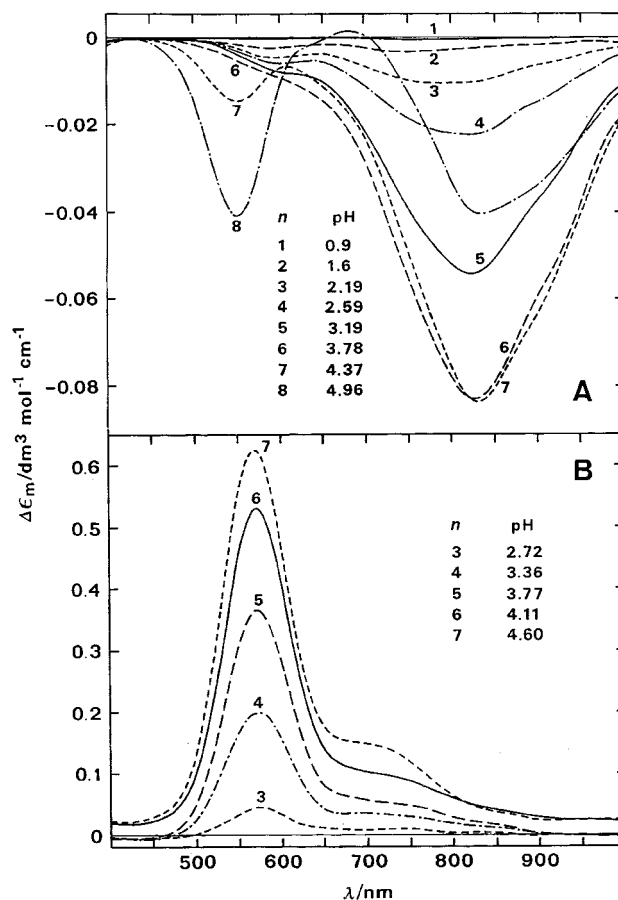
equatorial rather than axial donor ligands. Asymmetric deviations of ligating atoms from regular polyhedra (*asymmetric distortions*) may also make a significant contribution to the CD spectrum,[32,33] particularly in VO^{2+} complexes.

In these systems several optically active species may contribute at each pH, so extracting structural information from CD is not straightforward. In particular, the fact that in the pH range 3–8 $|\Delta\varepsilon_m|^{AspGly}$ are much greater than $|\Delta\varepsilon_m|^{GlyAsp}$ cannot be easily understood. One possibility is that the dominant complexes in the AspGly system (ML and MLH_{-1}) are more rigid, because of extra 'chelation'[49] (*e.g. via* hydrogen-bonding of a solvent water between two donor groups or the dipeptide behaving as tetradentate with one donor group axial): the configurational effect may then contribute to optical activity. Another explanation is a significant contribution to optical activity arising from *inherent dissymmetry* and *asymmetric distortions* for complexes ML and MLH_{-1} in the AspGly system. These effects may[32] be much stronger than the conformational or the vicinal effects. Vanadium in VO^{2+} may become an optically active centre, so most complexes here contain two dissymmetric centres. The structures presented correspond to one of two possible diastereomers: absolute configurations for oxovanadium, either C or A,[50] and for the α-carbon, L (*e.g.* discussion later for structure **17a**). Their stability may differ as found[51] by ^{51}V NMR for *e.g.* [V^VO(sal-L-aa)(dl$^-$)] (sal-L-aa = *N*-salicylidene-L-amino acidate of Gly, Ala, Val or Phe; dl$^-$ = monoanion of glycerol, ethane-1,2-diol or propane-1,3-diol), the trends observed being consistent with steric control. If this is the case for complexes ML and MLH_{-1} in the AspGly system, the
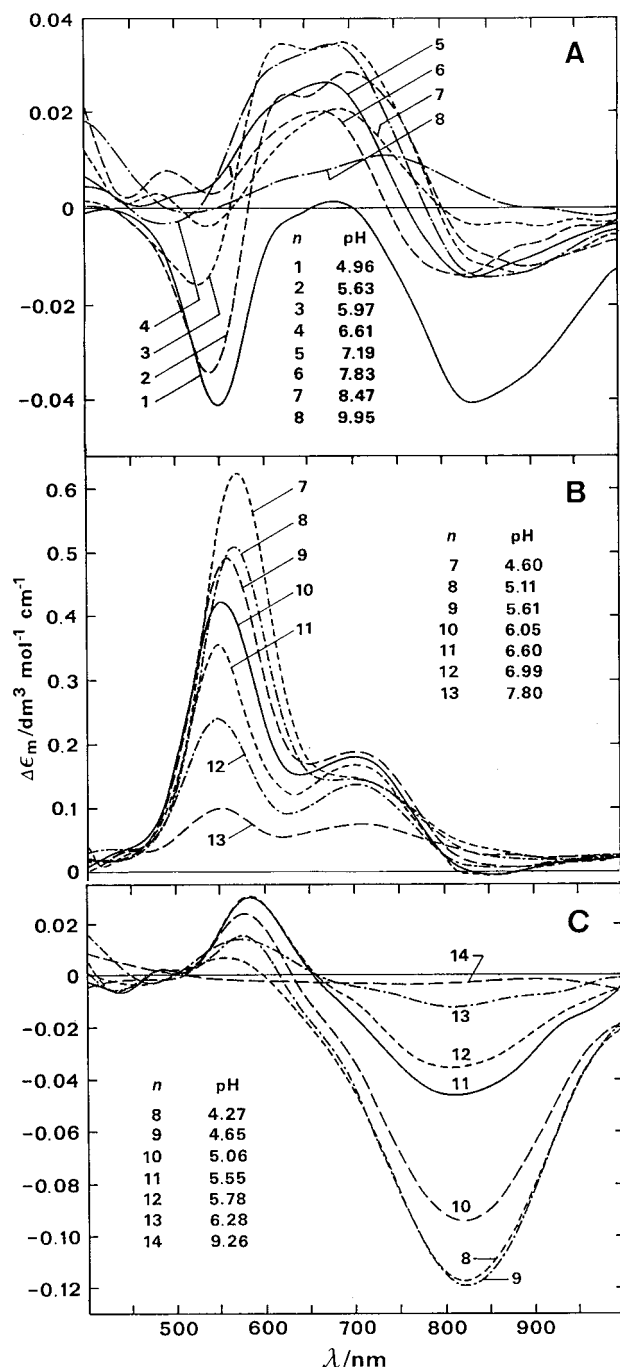
Fig. 5 Circular dichroism spectra of solutions containing: (A) GlyAsp and VO^{2+} with $L:M = 15.0:1$ and $C_{VO} \approx 0.016$–0.018 mol dm^{-3}, (B) AspGly and VO^{2+} with $L:M = 9.8:1$ and $C_{VO} \approx 0.006$–0.008 mol dm^{-3} and, (C) NacAsp and VO^{2+} with $L:M = 30.0:1$ and $C_{VO} \approx 0.008$–0.012 mol dm^{-3}. The pH corresponding to each spectrum is indicated. The ESR spectra corresponding to some of these solutions are in Fig. 2.

contributions of inherent dissymmetry, asymmetric distortions and finally that of the configurational effect may become important.

MLH$_2$ and ML′H

The stoichiometry MLH$_2$ (GlyAsp, AspGly) or ML′H (NacAsp, succinate) corresponds to structures with equatorially co-ordinated carboxylate (the terminal one in the case of GlyAsp and AspGly). The pattern of the VIS and CD spectra of this stoichiometry resembles spectra 2 of Fig. 3(A) and 4(A), and those for the corresponding VO^{2+} complexes of various amino acids[1–6] and simple dipeptides.[9,16] For GlyAsp and NacAsp, co-ordination involves the CO_2^- group near the

asymmetric centre, the CD showing its characteristic pattern (Fig. 3 and Table 2): for AspGly it involves the Gly residue, the CD being therefore extremely weak at pH 1–2.

Chasteen's method[24] (eqn. 3) gives $g_\parallel^{est} \approx 1.953$ and $A_\parallel^{est} \approx 180 \times 10^{-4}$ cm^{-1} for this geometry. Consequently, the values in Table 2 agree with those obtained for solutions containing mostly MLH$_2$ (and ML$_2$H$_4$) in the case of GlyAsp and AspGly, or ML′H (and ML$_2'$H$_2$) in the case of NacAsp and succinic acid.

$$VO^{2+} + H_2L \xrightarrow{K_{CO_2^-}} VO(H_2L)^{2+} \qquad (4A)$$

$$VO^{2+} + HL'^- \xrightarrow{K'_{CO_2^-}} VO(HL')^+ \qquad (4B)$$
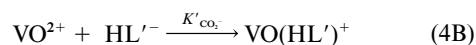
MLH or ML′ and ML$_2$H$_3$ or ML$_2'$H

In both MLH and ML′ the basic binding mode is probably chelation *via* both carboxylate groups. Derived equilibrium constants β_1^+ and β_1^* for MLH (GlyAsp, AspGly and Asp) or ML′, and also for corresponding complexes of some reference ligands, are in the second row of Table 4. The data show that 7-membered chelate formation is less favoured, log $\beta_1^* = -3.8$, than the 6-membered dicarboxylate chelate in the malonic acid system (log $\beta_1^* = -1.99$). The appropriate derived constants log β_1^* for NacAsp and succinic acid are ≈ -5 and -6, respectively, revealing important stabilisation for GlyAsp and AspGly complexes. This can very likely be explained by the co-ordination of O_{amide} of the peptides. For several plausible structures no strain is apparent and the amide group remains planar (*e.g.* **4**–**9**). This is the case of **4** for GlyAsp and **5**–**7** for AspGly. For AspGly, structures **6** and **7** and others containing two "free" equatorial positions are discarded; in fact, if they corresponded to MLH there would be no obvious reason for the absence of ML$_2$H$_3$ (or dimeric complexes where the equatorial positions occupied by W and/or Y could be shared with donor groups from the ligand of a second complex). Therefore MLH probably corresponds to **5** although the tridentate equatorial co-ordination is not apparent in the values of β_1^+ and β_1^*. For ML′ (NacAsp or succinic) the structures can correspond to **8** and/or **9**.

Structures for ML$_2$H$_3$ (GlyAsp) or ML$_2'$H (NacAsp or succinic) can be regarded as comprising those for MLH or ML′ plus a monodentate carboxylate group from a second ligand. Therefore, in the schematic structures here (*e.g.* **4**, **8** or **9**), X represents either H_2O or a RCO_2^- ligand. The spin-Hamiltonian parameters for ML$_2$H$_3$ or ML$_2'$H [$g_\parallel^{exptl} \approx 1.938$ and $A_\parallel^{exptl} \approx (173$–$174) \times 10^{-4}$ cm^{-1}] indicate equatorial co-ordination of three carboxylate groups, or two carboxylate groups and one O_{amide}; therefore structure **4**, **8** or **9** (and other isomers) is consistent with the ESR data. The pattern of CD expected for MLH (GlyAsp) and ML′ (NacAsp), and ML$_2$H$_3$ (GlyAsp) and ML$_2'$H, is the same; therefore, the dominant dissymmetric factors persist in corresponding stoichiometries in these systems, *i.e.* if, say, structure **4** is correct for GlyAsp, then for NacAsp the structure would correspond to **9**. However it is not yet possible to decide which geometry (**4**, **8**, **9** or some other) actually predominates.

ML (AspGly)

The pK values for the formation of ML stoichiometries are included in the fourth row of Table 4. While for NacAsp, succinic and malonic acids the pK values correspond to the deprotonation/co-ordination of a carboxylate group, for AspGly and L-Asp this corresponds to a similar process for the NH_3^+ group. The equatorial co-ordination of the NH_2 group of AspGly is indicated by the ESR spectra of Fig. 2(B), and by the spin-Hamiltonian parameters obtained for ML (Table 2). The

Table 3 Structures, corresponding $A_\parallel^{est}$, $g_\parallel^{est}$ [eqn. (3)],[a] stoichiometries and comment about expected origin for the optical activity for complexes that may form in solutions containing oxovanadium(IV) and GlyAsp, AspGly, NacAsp or succinic acid (see text)
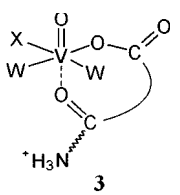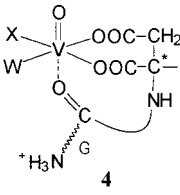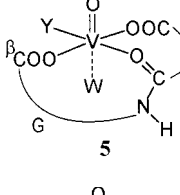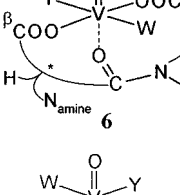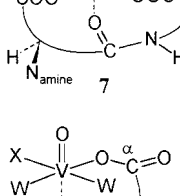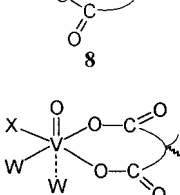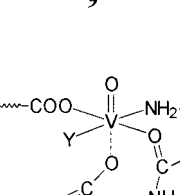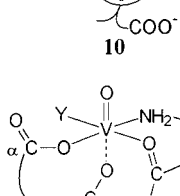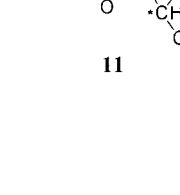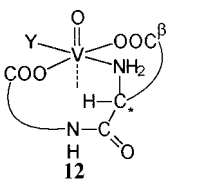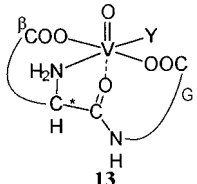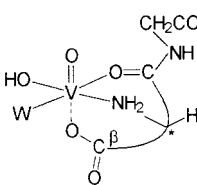
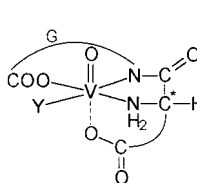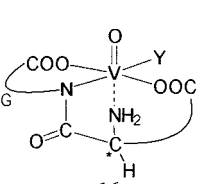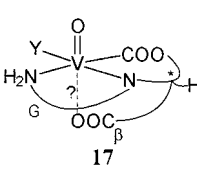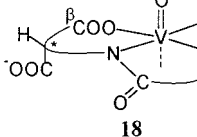| Schematic representation[b]	$A_\parallel^{est} \times 10^4/cm^{-1}$ ($g_\parallel^{est}$)	Stoichiometry (and comments)[c]
3	**a** X = H_2O 180 (1.935)	MLH_2 (GlyAsp or AspGly) (optical activity induced by the vicinal effect through the CO_2^- group)
	b X = $O_{carboxylate}$ 177 (1.937)	ML_2H_4 (GlyAsp or AspGly)
4	**a** X = H_2O 177 (1.937)	MLH (GlyAsp) (optical activity induced by the vicinal effect through the CO_2^- groups, and by the conformational effect)
	b X = $O_{carboxylate}$ 174 (1.939)	ML_2H_3 (GlyAsp)
5	**a** Y = H_2O 175 (1.939)[d]	MLH (AspGly) (optical activity induced by the vicinal effect throught the β-CO_2^- and $C=O_{amide}$, and by the conformational effect)
	b Y = OH^- 168 (1.946)[d]	MLH_{-1} (AspGly)
6	**a** Y = H_2O 174 (1.939)[d]	MLH (AspGly) [Optical activity induced by the vicinal effect through the β-CO_2^- (low) and $C=O_{amide}$ (very low) and by the conformational effect]
	b Y = OH^- 167 (1.946)[d]	MLH_{-1} (AspGly)
7	**a** Y = H_2O 174 (1.939)	MLH (AspGly) [optical activity induced by the vicinal effect through the β-CO_2^- (low) and $C=O_{amide}$ (very low), and by the conformational effect]
	b Y = OH^- 167 (1.946)	MLH_{-1} (AspGly)
8	**a** X = H_2O 180 (1.935)	MLH (AspGly) or ML′ (NacAsp or succinic[e]) [optical activity induced by the vicinal effect through the α-CO_2^- and β-CO_2^- (low) and by the conformational effect]
	b X = $O_{carboxylate}$ 174 (1.939)	ML_2H_3 (AspGly) or $ML_2′H$ (NacAsp or succinic[e])
9	**a** X = H_2O 177 (1.937)	MLH (AspGly) or ML′ (NacAsp or succinic[e]) [optical activity induced by the vicinal effect through the α-CO_2^- and β-CO_2^- (low) and by the conformational effect]
	b X = $O_{carboxylate}$ 170 (1.944)	ML_2H_3 (GlyAsp) or $ML_2′H$ (NacAsp or succinic[e])
10	**a** Y = H_2O 172 (1.942)	ML_2H (GlyAsp) [optical activity induced by the vicinal effect through the NH_2 (low), $C=O_{amide}$ (low) and axial CO_2^- (low), and by the conformational effect]
	b Y = OH^- 165 (1.950)	ML_2 (GlyAsp)
11	**a** Y = H_2O 172 (1.942)	ML_2H (GlyAsp) [optical activity induced by the vicinal effect through the NH_2 (low), $C=O_{amide}$ (low) and α-CO_2^- and by the conformational effect]
	b Y = OH^- 165 (1.950)	ML_2 (GlyAsp)

Table 3 (*Contd.*)

Schematic representation[b]	$A_{\parallel}^{est} \times 10^4/cm^{-1}$ ($g_{\parallel}^{est}$)	Stoichiometry (and comments)[c]
12	**a** Y = H$_2$O 171 (1.942)	ML (AspGly) [optical activity induced by the vicinal effect through the NH$_2$ and β-CO$_2^-$ (low) and by the conformational effect]
	b Y = OH$^-$ 164 (1.950)	MLH$_{-1}$ (AspGly)
13	**a** Y = H$_2$O 171 (1.942)	ML (AspGly) [optical activity induced by the vicinal effect through β-CO$_2^-$, NH$_2$ and C=O$_{amide}$ (low), and by the conformational, asymmetric distortion[f] and configurational effects]
	b Y = OH$^-$ 164 (1.950)	MLH$_{-1}$ (AspGly)
14	**a** Y = H$_2$O 175 (1.940)	MLH$_{-1}$ (AspGly) (optical activity induced by the vicinal effect through C=O$_{amide}$ and NH$_2$, and by the conformational effect)
	b Y = OH$^-$ 168 (1.947)	
15	**a** Y = H$_2$O ≈163[g] (≈1.950)[g]	MLH$_{-1}$ (AspGly) [optical activity induced by the vicinal effect through (CO)N$_{amide}$ and NH$_2$, by the conformational (?), asymmetric distortion[f] and configurational effects]
	b Y = OH$^-$ ≈158[g] (≈1.960)[g]	MLH$_{-2}$ (AspGly)
16	**a** Y = H$_2$O ≈165[g] (≈1.950)[g]	MLH$_{-1}$ (AspGly) [optical activity induced by the vicinal effect through (CO)N$_{amide}$ and β-CO$_2^-$, conformational, configurational and asymmetric distortion[f] effects]
	b Y = OH$^-$ ≈158[g] (≈1.957)[g]	MLH$_{-2}$ (AspGly)
17	**a** Y = H$_2$O ≈162[g] (≈1.953)[g]	MLH$_{-1}$ (GlyAsp) [optical activity induced by the vicinal effect through N$_{amide}$ and α-CO$_2^-$ and by the conformational (?), configurational and asymmetric distortion[f] effects]
	b Y = OH$^-$ ≈158[g] (≈1.960)[g]	MLH$_{-2}$ (GlyAsp)
18	**a** Y = H$_2$O ≈162[g] (≈1.953)[g]	MLH$_{-1}$ (GlyAsp) [optical activity induced by the vicinal effect through N$_{amide}$ and β-CO$_2^-$ (low), by the conformational effect and asymmetric distortions[f]]
	b Y = OH$^-$ ≈158[g] (≈1.960)[g]	MLH$_{-2}$ (AspGly)

[a] The $A_{\parallel}^{est}$ presented were calculated using eqn. (3) and the $g_{\parallel}^{est}$ using an equivalent equation. In these estimates we assume that ligands co-ordinated in axial position have no influence on the spin-Hamiltonian parameters. The $A_{\parallel}$ and $g_{\parallel}$ donor group contributions presented by Chasteen[24] assume axial co-ordination of water. [b] The glycine residue is normally indicated with a G; the CO$_2^-$ group of the side chain of the aspartic residue with a β. [c] The optical activity induced by the vicinal effect through NH$_2$ or CO$_2^-$ of glycine residues, or from groups co-ordinated in axial position, is expected to be low. [d] Assuming the contribution of O$_{amide}$ in eqn. (3) is 174.7×10^{-4} cm^{-1} as presented by Pecoraro and co-workers.[26] [e] No optical activity for the succinato complexes. [f] The effect of asymmetric distortions (see text) may be important whenever there are distortions in the otherwise symmetric regular structures of complexes. As a whole these distortions must be dissymmetric.[1–6,32,33] [g] Assuming that the contributions of N$_{amide}$ to $A_{\parallel}$ and $g_{\parallel}$ are 136×10^{-4} cm^{-1} and 1.983, respectively.[16,28,29]

CD and VIS spectra for ML approximately correspond to spectra 7 of Figs. 4(B) and 3(B), respectively. Structure **12a** or **13a** could correspond to ML. For **12a** the axial co-ordination of a water molecule is apparently precluded by the *a*-proton of the Asp residue. There is no significant strain in tetradentate co-ordination of AspGly and we propose **13a** as the structure of the AspGly complex corresponding to ML stoichiometry.

ML$_2$H$_2$ and ML$_2'$

The pK values for the formation of ML$_2'$ from ML$_2'$H or ML$_2$H$_2$ from ML$_2$H$_3$ are included in the fifth row of Table 4, being in the range 3.2–5.2. Comparing these values with the corresponding pK_{a2} of the 'free' ligands, no significant decrease in the pK of the carboxylic groups is observed in ML$'_2$H or ML$_2$H$_3$ complexes. The changes observed in the ESR, VIS and

Table 4 Derived equilibrium constants for VO^{2+} complex formation, partial processes of the ligands studied and some related compounds

		GlyAsp	AspGly	NacAsp	Succinic acid	GlyGly[9]	Ala[1]	Gly[10]	Malonic acid[35]	Aspartic acid[5]	AspGly (Cu)[41]	GlyAsp (Cu)[40]
Monodentate CO_2^- co-ordination[a]	$\log K_{CO_2^-}$	2.5	1.9	1.7	2.0	1.8	1.19	1.17	1.18	≈1.9	—	—
Bidentate $^-O_2C\cdots CO_2^-$ co-ordination[b]	$\log \beta_1^+$	3.16 (7-m.r.)	2.53 (7-m.r.)	2.7 (7-m.r.)	3.20 (7-m.r.)	—	—	—	5.6 (6-m.r.)	2.8 (7-m.r.)	2.1	2.1
	$\log \beta_1^*$	−3.72	−3.86	−4.9	−5.97	—	−5.62	−5.60	−1.99	−3.22	—	−5.04
Bidentate $(^-O_2C\cdots CO_2^-)_2$ co-ordination[c]	$\log \beta_2^+$	5.8 (7-m.r.)	—	5.0 (7-m.r.)	5.6 (7-m.r.)	—	—	—	9.5 (6-m.r.)	≈5.0 (7-m.r.)	—	—
	$\log \beta_2^*$	−7.98		−10.2	−12.7		−12.6	−12.4		−7.0		
$MLH \rightleftharpoons ML + H^+$ or	pK	—	4.0							≈3.5	3.5	3.8
$ML'H \rightleftharpoons ML' + H^+$				3.5	4.0		4.3	4.3	≈0.6			
$ML_2H_3 \rightleftharpoons ML_2H_2 + H^+$ or	pK	4.1	—							≈3.2		
$ML'_2H \rightleftharpoons ML'_2 + H^+$				4.6	5.2	—	5.2	4.8	—		—	—
$ML_2H_2 \rightleftharpoons ML_2H + H^+$ or	pK	5.4	—							≈3.5	—	—
$ML'_2 \rightleftharpoons ML'_2H_{-1} + H^+$				—	—	—	8.0	7.7	—			
$ML \rightleftharpoons MLH_{-1} + H^+$ or	pK	—	5.6			pK^{amide} ≈7				6–7	pK^{amide} 4.9	pK^{amide} 4.8
$ML' \rightleftharpoons ML'H_{-1} + H^+$				—	—		≈5.3	≈5.2	5.1			

[a] Ligand is protonated except at the carboxylate which co-ordinates; $K_{CO_2^-}$ is defined for reactions corresponding to eqns. (4A) (GlyAsp, AspGly, Asp) and (4B) for the rest of the ligands. [b] Ligand is protonated at amino group: β^+ is defined for reactions $VO + LH \rightleftharpoons VOLH$ (GlyAsp, AspGly and Asp) or $VO + L' \rightleftharpoons VOL'$ (rest of the ligands). The basicity corrected β_1^* is defined for $VO + H_3L \rightleftharpoons VOHL + 2H^+$ (GlyAsp, AspGly and Asp) or $VO + H_2L' \rightleftharpoons VOL' + 2H'$ (rest of the ligands); 7-m.r., 6-m.r. = 7- and 6-membered ring respectively. [c] The same as for footnote b but for bis complexes: β_2^+ is defined for reactions $VO + 2HL \rightleftharpoons VO(LH)_2$ (GlyAsp, AspGly and Asp) or $VO + 2L' \rightleftharpoons VOL'_2$ (rest of the ligands). The basicity corrected β_2^* is defined for $VO + 2H_3L \rightleftharpoons VO(HL)_2 + 4H^+$ (GlyAsp, AspGly and Asp) or $VO + 2H_2L' \rightleftharpoons VOL'_2 + 4H^+$ (rest of the ligands).

CD spectra as pH is increased for GlyAsp, NacAsp and succinic acid do however suggest that the co-ordination geometries of the complexes alter. This may be explained assuming that the O atoms of the second CO_2^- group in ML'_2 or ML_2H_2 also co-ordinate to VO^{2+}. The co-ordination geometries either involve all carboxylate O atoms equatorial or three equatorial and one axial (in the case of GlyAsp with possibly O_{amide} equatorial). The ESR parameters for ML'_2 or ML_2H_2 cannot be determined accurately but the approximate values presented in Table 2 are consistent with these geometries if the contributions of $O_{carboxylate}$ and O_{amide} are similar.

Formation constants β_2^+ (corrected for the protonation of the NH_3^+ group: $\beta_2^+ = \beta_{122}/\beta_{011}^2$) for complexes involving two 7-membered chelate rings co-ordinated by carboxylate groups (assuming these are the donor groups) are $\approx 10^5$ (third row of Table 4), while for malonate, which involves two 6-membered chelate rings, $\beta_{120} \approx 10^{9.5}$. Basicity corrected formation constants β^*, defined assuming ligands totally protonated (for H_3L ligands: $\beta_2^* = \beta_{122}/\beta_{013}^2$ and for H_2L' ligands $\beta_2^* = \beta_{120}/\beta_{012}^2$) are significantly higher for GlyAsp and Asp than for NacAsp and succinic acid. As for MLH and ML_2H_3 there is extra stabilisation for GlyAsp complexes possibly due to the co-ordination of O_{amide} of one of the ligands.

The VIS spectra for ML_2H_2 (GlyAsp) and ML_2' (NacAsp and succinic acid) approximately correspond to spectrum 7 of Fig. 3(A). The CD spectrum is dominated by a relatively intense and negative band I (GlyAsp and NacAsp: $\lambda_{max} \approx 820–830$ nm), a negative band II at $\lambda_{max} \approx 550$ nm (GlyAsp) or a relatively weak and positive band II at $\lambda_{max} \approx 575$ nm (NacAsp); all these differ from the corresponding bands in the L-Asp system: this is also in accordance with its different binding mode.

ML_2H (GlyAsp)

The pK for the process $ML_2H_2 \longrightarrow ML_2H + H^+$ (sixth row of Table 4) is 5.4 (≈ 3.5 for L-Asp). This is not the deprotonation of equatorial water as ML_2H_2 has no such group. While this pK gives little change in ESR, the pattern of CD shows drastic changes from pH 4.5 to 6.5 due to the formation of ML_2H and MLH_{-1}. This may involve changes in the co-ordination of the equatorial and axial donor functions. The spin-Hamiltonian parameters for ML_2H (Table 2) practically coincide with those expected for four equatorially co-ordinated $O_{carboxylate}$ and/or O_{amide} atoms,[25,26] so the geometry may be either $(CO_2^-)_4$, $(CO_2^-)_3(O_{amide})$ or $(CO_2^-)_2(O_{amide})_2$. Analysing the CD spectra for L:M 15 and 30:1 in the pH range 4.5–6.5 (Fig. 5) we expect for ML_2H a pattern $-,+,-$ with $\lambda_{max} \approx 530 \pm 20$ nm (band II), $\approx 630 \pm 20$ (band IB) and $\approx 840 \pm 30$ nm (band IA). Therefore the symmetry for this complex is low and the structure such that bands IA and IB are separate. Axial co-ordination of OH^- is not expected to promote change in the CD. Alternative co-ordination geometries for ML_2H_2 are 10a and 11a (Table 3: Y = H_2O). These correspond to $A_{\parallel}^{est} \approx 172 \times 10^{-4}$ cm^{-1} and could help explain the low $\Delta\varepsilon_m$ values for the GlyAsp system relative to AspGly, as the equatorial NH_2 and $C=O_{amide}$ are far from the asymmetric carbon and a low vicinal effect is expected.

It might be surprising that formation of bis complexes is disfavoured with AspGly, although N-terminal Asp offers a β-Ala chelation site. However, this is not favoured for VO^{2+} which binds N-donors rather weakly. Unlike GlyAsp, chelating O-donor sites, including carboxylate groups (strong binding functions for VO^{2+}), are not similarly available in AspGly.

MLH_{-1}, $ML'H_{-2}$ and MLH_{-2}

The pK values for the formation of MLH_{-1} (seventh row in Table 4) for the dipeptides can either correspond to the deprotonation/co-ordination of $N_{peptide}$, or to the deprotonation of an equatorially coordinated water molecule. These two processes correspond to the formation of complexes such as 5b, 6b, 7b, 12b, 13b, or 14–18 (Table 3).

The stoichiometry MLH_{-2} (GlyAsp) probably corresponds to a co-ordination geometry such as 17b (possibly OH^- axial instead of CO_2^-). For L:M = 30:1, maximum $|\Delta\varepsilon_m|$ are found at pH ≈ 9.5, conditions where MLH_{-2} would dominate CD spectra for GlyAsp; the ESR and CD spectra similarly resemble those for the corresponding complexes with AlaAla and GlyAla [ESR: $A_{\parallel}^{exptl} = (161 \pm 1) \times 10^{-4}$ cm^{-1}, $g_{\parallel} = 1.954 \pm 0.004$. CD spectra: band II, $\lambda_{max} \approx 500$ nm, $\Delta\varepsilon < 0$; band I, $\lambda_{max} \approx 720–750$ nm, $\Delta\varepsilon > 0$].[16] This is why structure 17b is assigned to MLH_{-2} and not 18. This is also consistent with 5-membered rings being more stable than 6-membered ones.

Over the pH range 6.5–8 where MLH_{-1} (GlyAsp) is predominant, as pH is increased the ESR spectra change little apart from decreasing intensity, but the CD shows changes due to the processes of Scheme 2. Some of these equilibria take time to establish making the exact pattern of CD bands for MLH_{-1} elusive. The band pattern $-,+,-$ at L:M = 15:1 may be due to the optically active oligomeric species: increasing L:M, the CD spectra in the pH range 7–8.5 change towards a $-,+$ pattern. So MLH_{-1} and MLH_{-2} may well have identical CD band patterns, i.e. both like the corresponding complexes in the AlaAla and GlyAla systems;[16] the co-ordination geometry for MLH_{-1} therefore probably corresponds to 17a, although it is not possible to rule out geometries such as $(CO_2^-, NH_2, CO_2^-, OH^-)_{equatorial}$. The few results available for the oligomeric optically active species that form make it impossible to predict their binding modes. Assuming 17a corresponds to the geometry of MLH_{-1} in the GlyAsp + VO^{2+} system, and taking into account that now the vanadium atom is an asymmetric centre, two diastereomers may be considered.

17a*
(V chirality[50]: A. α-C:L)

17a
(V chirality[50]: C. α-C:L)
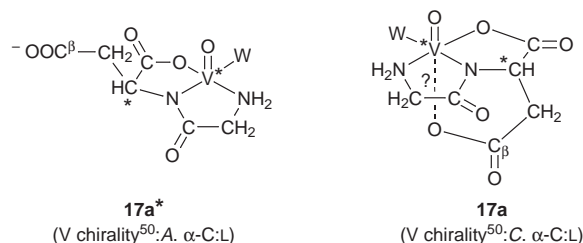
The geometry for both complexes corresponds to a distorted polyhedron and the contributions of inherent dissymmetry and asymmetric distortions to the optical activity will roughly cancel if both diastereomers are present in equal concentrations; however, if in 17a the β-CO_2^- is co-ordinated axial, this makes 17a slightly more stable than 17a*, these contributions to optical activity and its magnitude then depending on the relative concentration of the diastereomers. Similar comments apply to most structures included in Table 3.

For the MLH_{-1} (and MLH_{-2}) stoichiometries in the AspGly system, besides 5b, 6b, 7b, the following basic binding modes may be envisaged all compatible with the ESR: $(CO_2^-, N^-_{amide}, NH_2, Y)_{equatorial}$, e.g. 15, $(CO_2^-, NH_2, CO_2^-, Y)_{equatorial}$, e.g. 12, 13 or $(CO_2^-, N^-_{amide}, CO_2^-, Y)_{equatorial}$, e.g. 16. The present results and earlier data do not suffice to define the geometry for MLH_{-1} and MLH_{-2} stoichiometries, 15 and 16 corresponding to what is normally assumed for Cu^{2+} complexes.[30,31] Structure 16 is more in agreement with the high $|\Delta\varepsilon_m|$ values obtained for the AspGly–VO^{2+} system [Fig. 5(B)]. In the GlyAsp system MLH_{-1} starts to form at pH higher than for AspGly; this may be due to its higher pK_{a2}, pK_{a3}, and to some steric factor making tetradentate co-ordination (e.g. 17a) unfavorable.

In solutions containing NacAsp and VO^{2+} [L:M = 15 or 30:1 e.g. Fig. 5(C)] the CD spectra for pH > 5 differ from those of GlyAsp in similar conditions, and the $|\Delta\varepsilon_m|$ values decrease for pH > 5–5.5. If N^-_{amide} co-ordinates, e.g.: $(CO_2^-, N^-_{amide}, CO_2^-, Y)_{equatorial}$, we would expect an increase in $|\Delta\varepsilon_m|$ with pH and lower values of $A_{\parallel}^{exptl}$ for $ML'H_{-2}$ (Table 2). These observations indicate that, for the NacAsp system, N^-_{amide} does not

co-ordinate, and that NH_2, although not a good anchor for VO^{2+}, is involved in co-ordination for the corresponding stoichiometries in the GlyAsp system (in agreement with our conclusions there). Therefore, the stoichiometry $ML'H_{-2}$ (NacAsp and succinic) possibly involves complexes where co-ordination is $(OH^-, OH^-, CO_2^-, H_2O)_{equatorial}$ and $(CO_2^-)_{axial}$, which corresponds to $A_\parallel^{est} \approx 168 \times 10^{-4}$ cm^{-1}. This and the extensive hydrolysis of oxovanadium(IV) are also compatible with the very low CD and ESR signal at pH > 7 for NacAsp + VO^{2+}.

The only evidence for the stoichiometry $ML'H_{-3}$ (succinic acid) is that a new ESR active species appears at pH $\approx$ 7 (see above) with $A_\parallel^{exptl} \approx (165 \pm 2) \times 10^{-4}$ cm^{-1}; this possibly corresponds to a geometry involving $(2CO_2^-, 2OH^-)_{equatorial}$ $(OH^-)_{axial}$. This would have $A_\parallel^{est} \approx 163 \times 10^{-4}$ cm^{-1} while geometries of the type $(CO_2^-, 3OH^-)_{equatorial}$ $(CO_2^-)_{axial}$ would give $A_\parallel^{est} \approx 159 \times 10^{-4}$ cm^{-1}.

Summarizing the behaviour of the studied dipeptides, in the weakly acidic range only the carboxylate, the peptide CO and amino groups (this latter being somewhat less favoured) participate in the metal ion binding. The position of the tridentate Asp residue in the peptide chain affects the co-ordination mode of the ligands: when Asp is C-terminal (GlyAsp) it rather behaves as a succinic acid favouring equatorial carboxylate chelation of two neighbouring groups with some involvement of the peptide CO in metal binding. In the N-terminal Asp dipeptide, AspGly, the involvement of either the peptide carbonyl or the terminal amino groups seems more essential, since the two carboxylates are much further apart.

For pH > 6–7 the dominant stoichiometries for the ESR and CD active complexes are MLH_{-1} and MLH_{-2}. Further, for GlyAsp the results indicate the basic binding mode: $(CO_2^-, N^-_{amide}, NH_2, Y)_{equatorial}$ with $Y = H_2O$ or OH^-. The axial co-ordination of the β-CO_2^- group is possible but unproven. The binding mode for AspGly differs, particularly the fact that, at least till L : M = 8 : 1, only 1 : 1 complexes form. The distinction in the mode of 1 : 1 attachment to the VO^{2+} ion of these isomeric dipeptides is a remarkable new property. Whereas with the 'spherical' copper(II) ion, the chelating stabilities of N-terminal GlyAsp[40] and C-terminal AspGly[41] are the same, with the lop-sided vanadyl ion they differ markedly.

Acknowledgements

References

1 J. Costa Pessoa, L. F. Vilas Boas, R. D. Gillard and R. J. Lancashire, *Polyhedron*, 1988, **7**, 1245.

2 J. Costa Pessoa, L. F. Vilas Boas and R. D. Gillard, *Polyhedron*, 1989, **8**, 1173.

3 J. Costa Pessoa, L. F. Vilas Boas and R. D. Gillard, *Polyhedron*, 1989, **8**, 1745.

4 J. Costa Pessoa, L. F. Vilas Boas and R. D. Gillard, *Polyhedron*, 1990, **9**, 2101.

5 J. Costa Pessoa, R. L. Marques, L. F. Vilas Boas and R. D. Gillard, *Polyhedron*, 1990, **9**, 81.

6 J. Costa Pessoa, J. L. Antunes, L. F. Vilas Boas and R. D. Gillard, *Polyhedron*, 1992, **11**, 1449.

7 J. Costa Pessoa, S. M. Luz, I. Cavaco and R. D. Gillard, *Polyhedron*, 1994, **13**, 3177.

8 J. Costa Pessoa, S. M. Luz and R. D. Gillard, *Polyhedron*, 1995, **14**, 1495.

9 J. Costa Pessoa, S. M. Luz and R. D. Gillard, *Polyhedron*, 1993, **12**, 2857.

10 I. Nagypál and I. Fábián, *Inorg. Chim. Acta*, 1982, **62**, 193.

11 H. Sakurai, Y. Hamada, S. Shimomura, S. Yamashita and K. Ishizn, *Inorg. Chim. Acta*, 1980, **46**, L119; H. Sakurai, S. Shimomura and K. Ishizn, *Inorg. Chim. Acta*, 1981, **55**, L67; H. Sakurai, Z. Taira and N. Sakai, *Inorg. Chim. Acta*, 1988, **151**, 85.

12 M. D. Sifri and T. L. Riechel, *Inorg. Chim. Acta*, 1988, **142**, 229.

13 A. Dess, G. Micera and D Sanna, *J. Inorg. Biochem.*, 1993, **52**, 275.

14 T. Kiss, P. Buglyó, G. Micera, A. Dessi and D. Sanna, *J. Chem. Soc., Dalton Trans.*, 1993, 1849.

15 K. Knüttel, A. Müller, D. Rehder, H. Vilter and V. Wittneben, *FEBS*, 1992, **302**, 11.

16 J. Costa Pessoa, S. M. Luz and R. D. Gillard, *J. Chem. Soc., Dalton Trans.*, 1997, 569.

17 M. Delfini, E. Gaggelli, A. Lepri and G. Valensin, *Inorg. Chim. Acta*, 1985, **107**, 87.

18 R. P. Ferrari, E. Laurenti, S. Poli and L. Casella, *J. Inorg. Biochem.*, 1992, **45**, 99.

19 E. G. Ferrer, P. A. Williams and E. J. Baran, *Biol. Trace Elem. Res.*, 1991, **30**, 175; *J. Inorg. Biochem.*, 1993, **50**, 253; P. A. Williams and E. J. Baran, *J. Inorg. Biochem.*, 1994, **54**, 75.

20 E. G. Ferrer, P. A. Williams and E. J. Baran, *Biol. Trace Elem. Res.*, 1996, **55**, 153; *Transition Met. Chem.*, 1997, **22**, 589.

21 L. Xiaoping and X. Yuanzhi, *Kexue Tongbao*, 1985, **30**, 340; L. Xiaoping and Z. Kangjing, *J. Crystallogr. Spectrosc. Res.*, 1986, **16**, 681.

22 J. Costa Pessoa, T. Gajda, S. M. Luz, T. Kiss, J. J. G. Moura and I. Torok, *J. Inorg. Biochem.*, 1997, **67**, 388.

23 L. F. Vilas Boas and J. Costa Pessoa, in *Comprehensive Coordination Chemistry*, eds. G. Wilkinson, R. D. Gillard and J. A. McCleverty, Pergamon, Oxford, 1987, vol. 3, pp. 453–583 and refs. therein.

24 N. D. Chasteen, in *Biological Magnetic Resonance*, eds. J. Lawrence, L. J. Berliner and J. Reuben, Plenum, New York, 1981, vol. 3, p. 53.

25 C. R. Cornman, E. P. Zovinka, Y. D. Boyajian, K. M. Geiser-Bush, P. D. Boyle and P. Singh, *Inorg. Chem.*, 1995, **34**, 4213.

26 B. J. Hamstra, A. L. P. Houseman, G. J. Colpas, J. W. Kampf, R. LoBrutto, W. D. Frasch and V. L. Pecoraro, *Inorg. Chem.*, 1997, **36**, 4866.

27 F. W. B. Einstein, R. J. Batchelor, S. J. Angus-Dunne and A. S. Tracey, *Inorg. Chem.*, 1996, 3, 1680.

28 A. J. Tasiopoulos, Y. G. Deligiannakis, J. D. Woolins, A. M. Z. Slawin and T. A. Kabanos, *Chem. Commun.*, 1998, 569.

29 A. J. Tasiopoulos, A. T. Vlahos, A. D. Keramidas, T. A. Kabanos, Y. G. Deligiannakis, C. P. Raptopoulou and A. Terzis, *Angew. Chem., Int. Ed. Engl.*, 1996, **35**, 2531.

30 R. Kuroda and Y. Saito, in *Circular Dichroism. Principles and Applications*, eds. K. Nakanishi, N. Berova and R. W. Woody, VCH, New York, 1994, ch. 9, pp. 223–225.

31 H. Sigel and R. B. Martin, *Chem. Rev.*, 1982, **82**, 385 and refs. therein.

32 N. C. Payne, *Inorg. Chem.*, 1973, **12**, 1151; K. Z. Suzuki, Y. Sasaki, S. Ooi and K. Saito, *Bull. Chem. Soc. Jpn.*, 1980, **53**, 1288; S. Okazaki and K. Saito, *Bull. Chem. Soc. Jpn.*, 1982, **55**, 785.

33 I. Cavaco, J. Costa Pessoa, M. T. Duarte, R. T. Henriques, P. M. Matias and R. D. Gillard, *J. Chem. Soc., Dalton Trans.*, 1996, 1989.

34 G. Gran, *Acta Chem. Scand.*, 1950, **4**, 559.

35 I. Nagypál and I. Fábián, *Inorg. Chim. Acta*, 1982, **61**, 109.

36 E. D. Moffat and R. I. Lytle, *Anal. Chem.*, 1959, **31**, 926.

37 T. Gajda, B. Henry and J. J. Delpeuch, *J. Chem. Soc., Dalton Trans.*, 1992, 2301.

38 L. Zekany and I. Nagypal, in *Computational Methods for the Determination of Stability Constants*, ed. D. Leggett, Plenum, New York, 1985.

39 R. P. Henry, P. C. H. Mitchell and J. E. Prue, *J. Chem. Soc., Dalton Trans.*, 1973, 1156.

40 A. Gergeley and E. Farkas, *J. Chem. Soc., Dalton Trans.*, 1982, 381.

41 I. Sóvágó, E. Farkas, T. Jankowska and H. Kozlowski, *J. Inorg. Biochem.*, 1993, **51**, 715.

42 A. E. Martell and R. M. Smith, *Critical Stability Constants*, Plenum, New York, 1974, vol. 1; 1977, vol. 3; 1982, vol. 5; 1989, vol. 6.

43 S. P. Singh and J. P. Tandon, *Acta Chim. Acad. Sci. Hung.*, 1974, **80**, 425.

44 A. E. Martell and R. J. Motekaitis, *Determination and Use of Stability Constants*, VCH, Weinheim, 1988, p. 197.

45 EPRPOW, L. K. White and R. L. Belford, University of Illinois (modified by L. K. White, N. F. Albanese and N. D. Chasteen, University of New Hampshire to include both Lorentzian and Gaussian line shape functions, an $I = 7/2$ nucleus, a 4th hyperfine interaction and multiple sites having different linewidths), 1978.

46 G. Micera and A. Dessi, *J. Inorg. Biochem.*, 1988, **33**, 99.

47 D. B. McPhail and B. A. Goodman, *J. Chem. Soc.*, *Faraday Trans.*, 1987, 3513.
48 L. Casella, M. Gullotti and A. Pintar, *Inorg. Chim. Acta*, 1988, **144**, 89.
49 R. D. Gillard, *J. Inorg. Nucl. Chem.*, 1964, **26**, 657; J. P. Mathieu, Contributions to the Study of Molecular Structure, (*Victor Henri Commem. Vol*), Désoer, Liège, 1947, p. 111.
50 G. J. Leigh (Editor), *Nomenclature of Inorganic Chemistry*, Blackwell Scientific Publications, Oxford, 1990, p. 186.
51 S. Mondal, S. P. Rath, K. K. Rajak and A. Chakravorty, *Inorg. Chem.*, 1998, **37**, 1713.

Paper 8/01888J